

Grassmannian Dimensionality Reduction Using Triplet Margin Loss for Universal Manifold Embedding Classification of 3D Point Clouds

Yuval Haitman^{*}, Joseph M. Francos^{*} and Louis L. Scharf[†]

^{*}Electrical & Computer Engineering Department, Ben-Gurion University, Beer-Sheva, Israel

[†] Department of Mathematics, Colorado State University, Fort Collins, CO, USA

April 18, 2022

Detection and Classification of 3-D Objects Undergoing Rigid Transformations

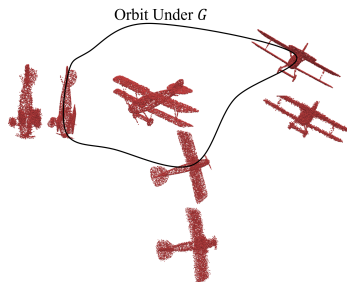
- Consider a 3-D object $s \in \{s_1, \dots, s_K\}$, and the *orbit* of equivalent observations formed by the action of the transformation group $G = SE(3)$ on s .

Detection and Classification of 3-D Objects Undergoing Rigid Transformations

- Consider a 3-D object $s \in \{s_1, \dots, s_K\}$, and the *orbit* of equivalent observations formed by the action of the transformation group $G = SE(3)$ on s .
- The set of possible observations on these equivalent objects is generally a manifold in the ambient space of observations.

Detection and Classification of 3-D Objects Undergoing Rigid Transformations

- Consider a 3-D object $s \in \{s_1, \dots, s_K\}$, and the *orbit* of equivalent observations formed by the action of the transformation group $G = SE(3)$ on s .
- The set of possible observations on these equivalent objects is generally a manifold in the ambient space of observations.
- In the presence of observation noise and random sampling patterns of the point clouds, the observations do not lie strictly on the manifold.



RTUME for Classification

- The Rigid Transformation Universal Manifold Embedding (RTUME)¹ provides a mapping from the orbit of observations on some object to a single low dimensional linear subspace of Euclidean space.

¹Amit Efraim and Joseph M Francos. "The Universal Manifold Embedding for Estimating Rigid Transformations of Point Clouds". In: *ICASSP 2019-2019 IEEE International Conference on Acoustics, Speech and Signal Processing (ICASSP)*. IEEE, 2019, pp. 5157–5161.

RTUME for Classification

- The Rigid Transformation Universal Manifold Embedding (RTUME)¹ provides a mapping from the orbit of observations on some object to a single low dimensional linear subspace of Euclidean space.
- This linear subspace is invariant to the geometric transformations and hence is a representative of the orbit.

¹Amit Efraim and Joseph M Francos. "The Universal Manifold Embedding for Estimating Rigid Transformations of Point Clouds". In: *ICASSP 2019-2019 IEEE International Conference on Acoustics, Speech and Signal Processing (ICASSP)*. IEEE, 2019, pp. 5157–5161.

RTUME for Classification

- The Rigid Transformation Universal Manifold Embedding (RTUME)¹ provides a mapping from the orbit of observations on some object to a single low dimensional linear subspace of Euclidean space.
- This linear subspace is invariant to the geometric transformations and hence is a representative of the orbit.
- In the classification set-up the RTUME subspace extracted from an experimental observation is tested against a set of subspaces representing the different object manifolds, in search for the nearest class.

¹Amit Efraim and Joseph M Francos. "The Universal Manifold Embedding for Estimating Rigid Transformations of Point Clouds". In: *ICASSP 2019-2019 IEEE International Conference on Acoustics, Speech and Signal Processing (ICASSP)*. IEEE, 2019, pp. 5157–5161.

Rigid Transformation Universal Manifold Embedding (RTUME)

- Let $h(\mathbf{x}), g(\mathbf{x})$ be two observations on the same object related by a rigid transformation:

$$h(\mathbf{x}) = g(\mathbf{R}\mathbf{x} + \mathbf{t}) \quad (1)$$

where $h(\mathbf{x}), g(\mathbf{x})$ are evaluated from the raw point cloud measurements using an $SE(3)$ -invariant function.

- We use the matrix representation of $SE(3)$ in homogeneous coordinates with right multiplication:

$$\mathbf{D}(\mathbf{R}, \mathbf{t}) = \begin{bmatrix} 1 & \mathbf{t}^T \\ \mathbf{0} & \mathbf{R}^T \end{bmatrix} \quad (2)$$

RTUME - Matrix Representation

RTUME Matrix

$$\mathbf{T}(h) = \begin{bmatrix} \int_{\mathbb{R}^3} w_1 \circ h(\mathbf{x}) d\mathbf{x} & \int_{\mathbb{R}^3} x_1 w_1 \circ h(\mathbf{x}) d\mathbf{x} & \dots & \int_{\mathbb{R}^3} x_3 w_1 \circ h(\mathbf{x}) d\mathbf{x} \\ & \vdots & & \\ \int_{\mathbb{R}^3} w_M \circ h(\mathbf{x}) d\mathbf{x} & \int_{\mathbb{R}^3} x_1 w_M \circ h(\mathbf{x}) d\mathbf{x} & \dots & \int_{\mathbb{R}^3} x_3 w_M \circ h(\mathbf{x}) d\mathbf{x} \end{bmatrix} \quad (3)$$

- $\{w_m\}_{m=1}^M$ are measurable functions aimed at generating many compandings of the observation.

RTUME - Matrix Representation

RTUME Matrix

$$\mathbf{T}(h) = \begin{bmatrix} \int_{\mathbb{R}^3} w_1 \circ h(\mathbf{x}) d\mathbf{x} & \int_{\mathbb{R}^3} x_1 w_1 \circ h(\mathbf{x}) d\mathbf{x} & \dots & \int_{\mathbb{R}^3} x_3 w_1 \circ h(\mathbf{x}) d\mathbf{x} \\ & & \vdots & \\ \int_{\mathbb{R}^3} w_M \circ h(\mathbf{x}) d\mathbf{x} & \int_{\mathbb{R}^3} x_1 w_M \circ h(\mathbf{x}) d\mathbf{x} & \dots & \int_{\mathbb{R}^3} x_3 w_M \circ h(\mathbf{x}) d\mathbf{x} \end{bmatrix} \quad (3)$$

- $\{w_m\}_{m=1}^M$ are measurable functions aimed at generating many compandings of the observation.
- The RTUME matrices of $h(\mathbf{x}), g(\mathbf{x})$ are related by:

$$\mathbf{T}(h) = \mathbf{T}(g)\mathbf{D}^{-1}(\mathbf{R}, \mathbf{t}) \quad (4)$$

- Since $\mathbf{T}(h)$ and $\mathbf{T}(g)$ are related by a right invertible linear transformation, the column space of $\mathbf{T}(g)$ and the column space of $\mathbf{T}(h)$ are identical.

Design of the RTUME Operator: TL-GDRUME

- Classifier performance highly depends on the choice of the set of functions composing the UME operator.
- Find the functions, that best separates the RTUME representation of each object from those of the other objects, while minimizing the distance between observations on the same object.

$$d_{pF}(\langle \mathbf{T}(Z) \rangle, \langle \mathbf{T}(X) \rangle) = \frac{1}{\sqrt{2}} \|\mathbf{P}_X - \mathbf{P}_Z\|_F = \|\sin \boldsymbol{\theta}\|_2 \quad (5)$$

Design of the RTUME Operator: TL-GDRUME

- Classifier performance highly depends on the choice of the set of functions composing the UME operator.
- Find the functions, that best separates the RTUME representation of each object from those of the other objects, while minimizing the distance between observations on the same object.

$$d_{pF}(\langle \mathbf{T}(Z) \rangle, \langle \mathbf{T}(X) \rangle) = \frac{1}{\sqrt{2}} \|\mathbf{P}_X - \mathbf{P}_Z\|_F = \|\sin \boldsymbol{\theta}\|_2 \quad (5)$$

- Using Grassmannian dimensionality reduction and metric learning scheme we derive TL-GDRUME: An analytic solution for designing the RTUME operators.

Level Set Representation

- Given an observation $X(\mathbf{u})$, $\mathbf{u} \in \mathbb{R}^3$ the level-set representation of $X(\mathbf{u})$ is:

$$X(\mathbf{u}) = \sum_{i=1}^Q q_i \mathcal{I}_i^X(\mathbf{u}) \quad (6)$$

where $\mathcal{I}_i^X(\mathbf{u})$ is the indicator function of the level-set of \mathbf{u} where $q_{i-1} \leq X(\mathbf{u}) \leq q_i$.

Level Set Representation

- Given an observation $X(\mathbf{u})$, $\mathbf{u} \in \mathbb{R}^3$ the level-set representation of $X(\mathbf{u})$ is:

$$X(\mathbf{u}) = \sum_{i=1}^Q q_i \mathcal{I}_i^X(\mathbf{u}) \quad (6)$$

where $\mathcal{I}_i^X(\mathbf{u})$ is the indicator function of the level-set of \mathbf{u} where $q_{i-1} \leq X(\mathbf{u}) \leq q_i$.

- The action of a measurable function w_m on the level-set representation of $X(\mathbf{u})$ is to map q_i to $w_m(q_i)$:

$$w_m(X(\mathbf{u})) = \sum_{i=1}^Q w_m(q_i) \mathcal{I}_i^X(\mathbf{u}) \quad (7)$$

Fundamental Universal Manifold Embedding (FUME)

- Using the level-set representation of $X(\mathbf{u})$ each term of the RTUME matrix $\mathbf{T}(X)$ becomes:

$$\mathbf{T}_{m,j} = \int_{\mathbb{R}^3} w_m \circ X(\mathbf{u}) u_j d\mathbf{u} = \sum_{i=1}^Q w_m(q_i) \underbrace{\int_{\mathbb{R}^3} \mathcal{I}_i^X(\mathbf{u}) u_j d\mathbf{u}}_{\mathbf{F}_{i,j}^X} = \sum_{i=1}^Q w_{m,i} \mathbf{F}_{i,j}^X \quad (8)$$

Fundamental Universal Manifold Embedding (FUME)

- Using the level-set representation of $X(\mathbf{u})$ each term of the RTUME matrix $\mathbf{T}(X)$ becomes:

$$\mathbf{T}_{m,j} = \int_{\mathbb{R}^3} w_m \circ X(\mathbf{u}) u_j d\mathbf{u} = \sum_{i=1}^Q w_m(q_i) \underbrace{\int_{\mathbb{R}^3} \mathcal{I}_i^X(\mathbf{u}) u_j d\mathbf{u}}_{\mathbf{F}_{i,j}^X} = \sum_{i=1}^Q w_{m,i} \mathbf{F}_{i,j}^X \quad (8)$$

- and

$$\mathbf{T}(X) = \mathbf{W}^T \mathbf{F}^X; \quad \mathbf{W}^T = \{w_{m,i}\} \in \mathbb{R}^{M \times Q} \quad (9)$$

Fundamental Universal Manifold Embedding (FUME)

- Using the level-set representation of $X(\mathbf{u})$ each term of the RTUME matrix $\mathbf{T}(X)$ becomes:

$$\mathbf{T}_{m,j} = \int_{\mathbb{R}^3} w_m \circ X(\mathbf{u}) u_j d\mathbf{u} = \sum_{i=1}^Q w_m(q_i) \underbrace{\int_{\mathbb{R}^3} \mathcal{I}_i^X(\mathbf{u}) u_j d\mathbf{u}}_{\mathbf{F}_{i,j}^X} = \sum_{i=1}^Q w_{m,i} \mathbf{F}_{i,j}^X \quad (8)$$

- and

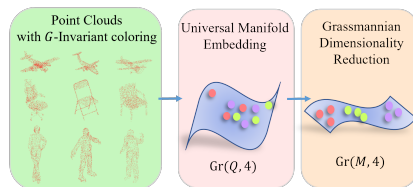
$$\mathbf{T}(X) = \mathbf{W}^T \mathbf{F}^X; \quad \mathbf{W}^T = \{w_{m,i}\} \in \mathbb{R}^{M \times Q} \quad (9)$$

- $\mathbf{F}^X = \{\mathbf{F}_{i,j}^X\} \in \mathbb{R}^{M \times Q}$ is the *Fundamental Universal Manifold Embedding* (FUME) matrix of $X(\mathbf{u})$.
- Since $M \leq Q$ the role of \mathbf{W} is to transform the subspace $\langle \mathbf{F}^X \rangle \in \text{Gr}(Q, 4)$ to the subspace $\langle \mathbf{G}^X \rangle \in \text{Gr}(M, 4)$.

Grassmannian Dimensionality Reduction

- Find $\mathbf{W} \in \mathbb{R}^{Q \times M}$ that jointly maps FUME subspaces from a Grassmannian with higher ambient space dimension to a Grassmannian with lower ambient space dimension.

$$\{\langle \mathbf{F}^k \rangle\}_{k=1}^N \in \text{Gr}(Q, 4) \xrightarrow{\mathbf{Y}^k = \mathbf{W}^T \mathbf{F}^k} \{\langle \mathbf{Y}^k \rangle\}_{k=1}^N \in \text{Gr}(M, 4) \quad (10)$$

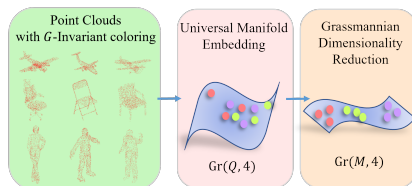


Grassmannian Dimensionality Reduction

- Find $\mathbf{W} \in \mathbb{R}^{Q \times M}$ that jointly maps FUME subspaces from a Grassmannian with higher ambient space dimension to a Grassmannian with lower ambient space dimension.

$$\{\langle \mathbf{F}^k \rangle\}_{k=1}^N \in \text{Gr}(Q, 4) \xrightarrow{\mathbf{Y}^k = \mathbf{W}^T \mathbf{F}^k} \{\langle \mathbf{Y}^k \rangle\}_{k=1}^N \in \text{Gr}(M, 4) \quad (10)$$

- \mathbf{W} is designed such that observations from the same orbit generate close together subspaces while those from different orbits generate far apart subspaces.

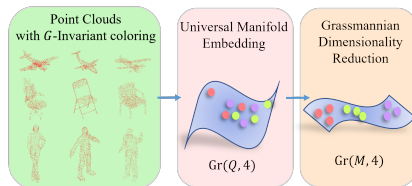


Grassmannian Dimensionality Reduction

- Find $\mathbf{W} \in \mathbb{R}^{Q \times M}$ that jointly maps FUME subspaces from a Grassmannian with higher ambient space dimension to a Grassmannian with lower ambient space dimension.

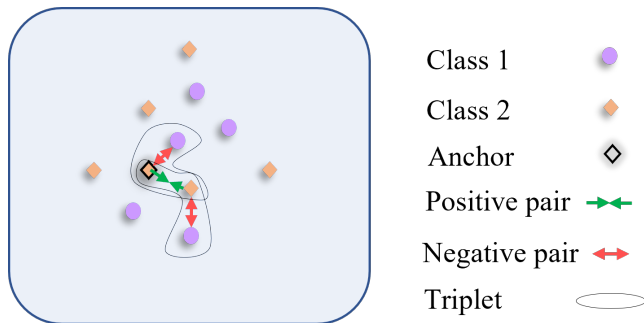
$$\{\langle \mathbf{F}^k \rangle\}_{k=1}^N \in \text{Gr}(Q, 4) \xrightarrow{\mathbf{Y}^k = \mathbf{W}^T \mathbf{F}^k} \{\langle \mathbf{Y}^k \rangle\}_{k=1}^N \in \text{Gr}(M, 4) \quad (10)$$

- \mathbf{W} is designed such that observations from the same orbit generate close together subspaces while those from different orbits generate far apart subspaces.
- A sufficient condition that guarantees all $\langle \mathbf{Y}^k \rangle$ are indeed on $\text{Gr}(M, 4)$ is that \mathbf{W} has a full column rank, or alternatively, that the columns of \mathbf{W} are orthonormal.



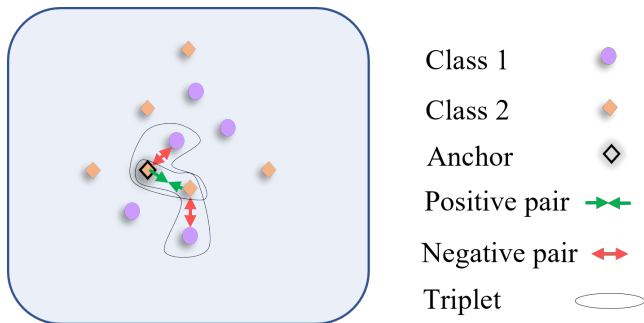
Metric Learning - Triplet Margin Loss

- We employ metric learning with hard-negative mining.



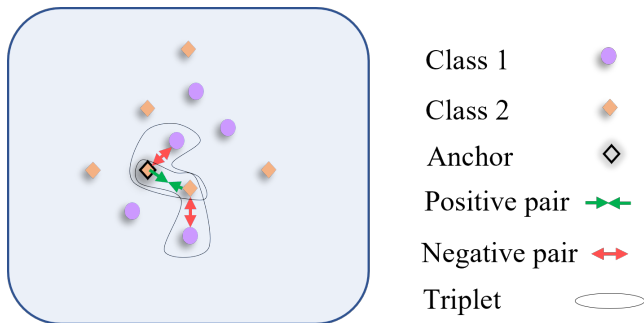
Metric Learning - Triplet Margin Loss

- We employ metric learning with hard-negative mining.
- Triplet loss jointly minimizes the distance between a given anchor and its positive match, while maximizing the distance to the hardest negative example.



Metric Learning - Triplet Margin Loss

- We employ metric learning with hard-negative mining.
- Triplet loss jointly minimizes the distance between a given anchor and its positive match, while maximizing the distance to the hardest negative example.
- Negative mining is applied both to the anchor and to its positive match.



TL-GDRUME Optimization of \mathbf{W}

- Given a training set of N labeled observations $\{X_i, k_i\}_{i=1}^N$, $k_i \in \{1, \dots, K\}$ and their corresponding FUME matrices $\{\mathbf{F}_i\}_{i=1}^N$.

TL-GDRUME Optimization of \mathbf{W}

- Given a training set of N labeled observations $\{X_i, k_i\}_{i=1}^N$, $k_i \in \{1, \dots, K\}$ and their corresponding FUME matrices $\{\mathbf{F}_i\}_{i=1}^N$.
- Examples are paired to positive (\mathcal{P}) and negative (\mathcal{N}) sets according to their class label, each set contains the indices of the appropriate examples.

TL-GDRUME Optimization of \mathbf{W}

- Given a training set of N labeled observations $\{X_i, k_i\}_{i=1}^N$, $k_i \in \{1, \dots, K\}$ and their corresponding FUME matrices $\{\mathbf{F}_i\}_{i=1}^N$.
- Examples are paired to positive (\mathcal{P}) and negative (\mathcal{N}) sets according to their class label, each set contains the indices of the appropriate examples.
- Points on the Grassmann manifold are represented by an orthogonal basis of the RTUME matrices $\{\mathbf{W}^T \mathbf{F}_i\}_{i=1}^N$ using *QR-decomposition*.

TL-GDRUME Optimization of \mathbf{W}

- Given a training set of N labeled observations $\{X_i, k_i\}_{i=1}^N$, $k_i \in \{1, \dots, K\}$ and their corresponding FUME matrices $\{\mathbf{F}_i\}_{i=1}^N$.
- Examples are paired to positive (\mathcal{P}) and negative (\mathcal{N}) sets according to their class label, each set contains the indices of the appropriate examples.
- Points on the Grassmann manifold are represented by an orthogonal basis of the RTUME matrices $\{\mathbf{W}^T \mathbf{F}_i\}_{i=1}^N$ using *QR-decomposition*.
- Distance between examples is measured by the projection Frobenius-norm on the Grassmannian:

$$D_{i,j}(\mathbf{W}) = d_{pF}^2(\langle \mathbf{Q}_i(\mathbf{W}) \rangle, \langle \mathbf{Q}_j(\mathbf{W}) \rangle) \quad (11)$$

TL-GDRUME Optimization of \mathbf{W}

TL-GDRUME Training

$$\min_{\mathbf{W} \in \mathbb{R}^{Q \times M}} L(\mathbf{W}) = \sum_{(i,j) \in \mathcal{P}} \left[m + D_{i,j}(\mathbf{W}) - \min_{k \in \mathcal{N}} D_{i,k}(\mathbf{W}) \right]_+ + \quad (12)$$
$$\left[m + D_{i,j}(\mathbf{W}) - \min_{k \in \mathcal{N}} D_{j,k}(\mathbf{W}) \right]_+$$

subject to $\mathbf{W}^T \mathbf{W} = \mathbf{I}_M$

- Since $\langle \mathbf{W}^T \mathbf{F}_i \rangle \in \text{Gr}(M, 4)$, distance values are bounded $D_{i,j}(\mathbf{W}) \in [0, 4]$ therefore a typical value for the margin m will be in this range.

²Nicolas Boumal et al. "Manopt, a Matlab toolbox for optimization on manifolds". In: *The Journal of Machine Learning Research* 15.1 (2014), pp. 1455–1459.

TL-GDRUME Optimization of \mathbf{W}

TL-GDRUME Training

$$\min_{\mathbf{W} \in \mathbb{R}^{Q \times M}} L(\mathbf{W}) = \sum_{(i,j) \in \mathcal{P}} \left[m + D_{i,j}(\mathbf{W}) - \min_{k \in \mathcal{N}} D_{i,k}(\mathbf{W}) \right]_+ + \quad (12)$$
$$\left[m + D_{i,j}(\mathbf{W}) - \min_{k \in \mathcal{N}} D_{j,k}(\mathbf{W}) \right]_+$$

subject to $\mathbf{W}^T \mathbf{W} = \mathbf{I}_M$

- Since $\langle \mathbf{W}^T \mathbf{F}_i \rangle \in \text{Gr}(M, 4)$, distance values are bounded $D_{i,j}(\mathbf{W}) \in [0, 4]$ therefore a typical value for the margin m will be in this range.
- $[\cdot]_+ = \max(0, \cdot)$.

²Nicolas Boumal et al. "Manopt, a Matlab toolbox for optimization on manifolds". In: *The Journal of Machine Learning Research* 15.1 (2014), pp. 1455–1459.

TL-GDRUME Optimization of \mathbf{W}

TL-GDRUME Training

$$\min_{\mathbf{W} \in \mathbb{R}^{Q \times M}} L(\mathbf{W}) = \sum_{(i,j) \in \mathcal{P}} \left[m + D_{i,j}(\mathbf{W}) - \min_{k \in \mathcal{N}} D_{i,k}(\mathbf{W}) \right]_+ + \quad (12)$$
$$\left[m + D_{i,j}(\mathbf{W}) - \min_{k \in \mathcal{N}} D_{j,k}(\mathbf{W}) \right]_+$$

subject to $\mathbf{W}^T \mathbf{W} = \mathbf{I}_M$

- Since $\langle \mathbf{W}^T \mathbf{F}_i \rangle \in \text{Gr}(M, 4)$, distance values are bounded $D_{i,j}(\mathbf{W}) \in [0, 4]$ therefore a typical value for the margin m will be in this range.
- $[\cdot]_+ = \max(0, \cdot)$.
- We solve an optimization problem on the Stiefel manifold (12) using manifold optimization toolbox Manopt².

²Nicolas Boumal et al. "Manopt, a Matlab toolbox for optimization on manifolds". In: *The Journal of Machine Learning Research* 15.1 (2014), pp. 1455–1459.

Experimental Setup and Results

- Evaluation on ModelNet40 point cloud dataset.

Sampling	Method	0.5 MR noise	0.8 MR noise
Uniform	FUME	0.85	0.83
	TL-GDRUME	0.93	0.91
Non - Uniform	FUME	0.83	0.81
	TL-GDRUME	0.92	0.90

Table: Accuracy comparison of FUME and TL-GDRUME on deformed ModelNet40 observations, uniformly and non-uniformly sampled, in the presence of noise.

Experimental Setup and Results

- Evaluation on ModelNet40 point cloud dataset.
- For each class we generated observations that differ by rigid transformation, additive noise and random sampling.

Sampling	Method	0.5 MR noise	0.8 MR noise
Uniform	FUME	0.85	0.83
	TL-GDRUME	0.93	0.91
Non - Uniform	FUME	0.83	0.81
	TL-GDRUME	0.92	0.90

Table: Accuracy comparison of FUME and TL-GDRUME on deformed ModelNet40 observations, uniformly and non-uniformly sampled, in the presence of noise.

Experimental Setup and Results

- Evaluation on ModelNet40 point cloud dataset.
- For each class we generated observations that differ by rigid transformation, additive noise and random sampling.
- The class of each observation in the test is determined to be the label of its nearest neighbor in the training set.

Sampling	Method	0.5 MR noise	0.8 MR noise
Uniform	FUME	0.85	0.83
	TL-GDRUME	0.93	0.91
Non - Uniform	FUME	0.83	0.81
	TL-GDRUME	0.92	0.90

Table: Accuracy comparison of FUME and TL-GDRUME on deformed ModelNet40 observations, uniformly and non-uniformly sampled, in the presence of noise.

Experimental Setup and Results

- Evaluation on ModelNet40 point cloud dataset.
- For each class we generated observations that differ by rigid transformation, additive noise and random sampling.
- The class of each observation in the test is determined to be the label of its nearest neighbor in the training set.
- We tested the classification performance under two different noise statistics and two sampling methods - uniform and non-uniform.

Sampling	Method	0.5 MR noise	0.8 MR noise
Uniform	FUME	0.85	0.83
	TL-GDRUME	0.93	0.91
Non - Uniform	FUME	0.83	0.81
	TL-GDRUME	0.92	0.90

Table: Accuracy comparison of FUME and TL-GDRUME on deformed ModelNet40 observations, uniformly and non-uniformly sampled, in the presence of noise.

Conclusions

- We have presented a novel approach for designing the RTUME of 3D point clouds towards optimizing its performance for detection and classification tasks.
- In the presence of observation noise and challenging sampling patterns, the observations do not lie strictly on the manifold and the resulting RTUME subspaces are noisy. Yet, TL-GDRUME provides highly accurate classification results compared to the naive FUME.

Thank You